An Improvement of BM3D Image Denoising and Deblurring Algorithm by Generalized Total Variation

Andrey Nasonov, Andrey Krylov
Laboratory of Mathematical Methods of Image Processing
Faculty of Computational Mathematics and Cybernetics
Lomonosov Moscow State University
Russia, Moscow, Leninsky gory, 1, BMK MGU
Email: kryl@cs.msu.ru

***Abstract*—In this work we propose a post-processing method for BM3D algorithm that has become a state-of-the-art image denoising and deblurring algorithm. Although BM3D algorithm produces results with high objective metrics values, it also adds noticeable high-frequency artifacts. We suppress these artifacts using second order Total Generalized Variation (TGV) algorithm. TGV algorithm is an extension of Total Variation denoising method but it does not tend to make images piecewise constant. We also suggest an efficient numerical scheme for TGV minimization. In order to validate the proposed idea, tests were performed on noisy real images and synthetic images with different levels of noise.**

***Index Terms*—image denoising, generalized total variation, BM3D, TGV**

I. Introduction

Most solutions of inverse problems and in particular of mathematical imaging problems are formulated as a solution of the minimization problem for a regularization functional

$$J(z) = \arg\min_z \left(\mathcal{F}(z) + \mathcal{R}(z)\right) \tag{1}$$

where $\mathcal{F}(z)$ represents data fidelity and $\mathcal{R}(z)$ is a regularization term.

In image restoration applications, the most common data fidelity term has a form of

$$\mathcal{F}(z) = \|Az - u\|^2, \tag{2}$$

where $A : z \to u$ is a direct operator, u is the given observation, z is the possibly error-prone data and $\|\cdot\|$ is an appropriately chosen Hilbertian norm.

Total Variation regularization

$$\mathcal{R}(z) = \alpha\|\nabla z\|_1 \tag{3}$$

has been used for image enhancement for almost 30 years [1] for its capability to preserve edges and is still relevant nowadays. For example, Total Variation is used as a loss function in convolutional neural networks [2], in image inpainting [3] and restoration [4].

However, Total Variation is also well known for producing staircase-like artifacts. A concept of Total Generalized Variation (TGV) has been recently proposed to be applied to images where the assumption that the image is piecewise constant is not valid. The Total Generalized Variation introduced in [5], [6] is a functional that is capable to measure, in some sense, image characteristics up to a certain order of differentiation. The difference between TV and second-order TGV regularization for image denoising is shown in Fig. 1.

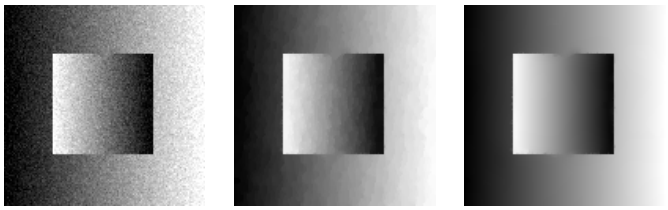

(a) Noisy image (b) TV regularization (c) TGV regularization

Fig. 1. The difference between TV and TGV regularization.

Recently proposed Block matching and 3D (BM3D) filtering added a new dimension to the study of denoising and deblurring [7], [8]. BM3D is the current state-of-the-art of denoising and is capable of achieving better denoising as compared to regularization-based methods. BM3D is very effective for additive white Gaussian noise removal. Its weak point is processing the images with structured noise. The modifications of BM3D have been developed for the case of correlated noise [9], [10]. However, the artifacts may still appear after BM3D deblurring because of noise structure.

In our work, we consider the improvement of BM3D algorithm by applying TGV denoising. New numerical scheme and TGV minimization algorithm are also proposed in the paper.

II. Generalized Total Variation

The second order TGV functional is formulated as [11]:

$$TGV^2_\alpha(z) = \min_v \alpha_1\|\nabla z - v\|_1 + \alpha_2\|\nabla v\|_1. \tag{4}$$

Here, the minimum is taken over the vector field v. The ratio of positive weights α_1 and α_2 provides a way of balancing between the first and second derivative of the function.

A. Auxiliary variable elimination

One of the issues with TGV stabilizer is developing the efficient minimization of (4). In order to simplify the minimization procedure, we eliminate the auxiliary variable v by calculating the second derivative directly:

$$TGV_{\alpha}^{2}(z) = \alpha_1 \|\nabla z\|_1 + \alpha_2 \|\nabla(\nabla z)\|_1. \tag{5}$$

The main reason of this transform is to avoid the calculation of gradient components and to use only gradient magnitude.

B. First order derivative calculation

Another issue with TV and TGV stabilizers is calculating the derivatives of image z. Proper numerical differentiation has a great influence on the result. For example, an ordinary derivative

$$|\nabla z|_{i,j} = \sqrt{z_x^2 + z_y^2} = \sqrt{(z_{i+1,j} - z_{i,j})^2 + (z_{i,j+1} - z_{i,j})^2}$$

could make the result anisotropic while symmetric derivative

$$|\nabla z|_{i,j} = \sqrt{\left(\frac{z_{i+1,j} - z_{i-1,j}}{2}\right)^2 + \left(\frac{z_{i,j+1} - z_{i,j-1}}{2}\right)^2}$$

does not use the value of the central pixel and could produce pattern artifact.

In simple Total Variation regularization (3) we set penalty on the sum of gradient magnitude, but we do not use the gradient components. Therefore, we can use the symmetrized derivative:

$$|\nabla z|_{i,j} = \sqrt{\tfrac{1}{2}((z_{i+1,j} - z_{i,j})^2 + (z_{i-1,j} - z_{i,j})^2 + \\ + (z_{i,j+1} - z_{i,j})^2 + (z_{i,j-1} - z_{i,j})^2)}. \tag{6}$$

Using the Total Variation in (6) directly is computationally inefficient due to square root and division calculation during the minimization procedure. A more computationally efficient way to represent the Total Variation is the following:

$$|\nabla z|_{i,j} = \frac{1}{2}(|z_{i+1,j} - z_{i,j}| + |z_{i-1,j} - z_{i,j}| + \\ + |z_{i,j+1} - z_{i,j}| + |z_{i,j-1} - z_{i,j}|). \tag{7}$$

The drawback of the approach (7) is anisotropy. A solution to this problem has been proposed in [12] as a Bilateral Total Variation functional that combines both efficiency and isotropy:

$$|\nabla z|_{i,j} = \sum_{s,t=-p}^{p} \frac{1}{\sqrt{s^2 + t^2}} |z_{i+s,j+t} - z_{i,j}|, |s| + |t| > 0. \tag{8}$$

Here we calculate the sum of moduli of partial derivatives. The value p controls the window size. Typical values are $p = 1$ and $p = 2$. We use $p = 1$ in order to reduce computational complexity.

C. Second order derivative calculation

The second order derivative is represented as a tensor:

$$\nabla(\nabla z) = \begin{bmatrix} z_{xx} & z_{xy} \\ z_{xy} & z_{yy} \end{bmatrix}.$$

We calculate the magnitude of the second order derivative in the same way as of the first order derivative:

$$|\nabla(\nabla z)|_{i,j} = \sum_{s,t=-p}^{p} \frac{1}{\sqrt{s^2 + t^2}} |z_{i+s,j+t} - \\ - 2z_{i,j} + z_{i-s,j-t}|, \quad |s| + |t| > 0. \tag{9}$$

III. Minimization algorithm

We use Sutskever-Nesterov accelerated gradient algorithm [13], [14] to minimize the regularization functional (1):

$$\begin{aligned} z^{(0)} &= 0 \\ v^{(0)} &= 0 \\ g^{(k+1)} &= \nabla J(z^{(k)} + \mu v^{(k)}) \\ v^{(k+1)} &= \mu v^{(k)} - \beta^{(k+1)} g^{(k+1)} \\ z^{(k+1)} &= z^{(k)} + v^{(k+1)} \end{aligned} \tag{10}$$

We choose the number of iterations N and the step $\beta^{(k)}$ in the following way

$$\beta^{(k+1)} = 25 \cdot 0.01^{k/N} \frac{P}{\|g^{(k+1)})\|_1},$$

where P is the image size (the number of pixels), and the pixel value range is within $[0, 255]$. This choice of the exponentially diminishing step leads to a non-changing image after about N iterations.

The accuracy of the algorithm depends on the number of iterations N and the momentum μ. Experiments have shown that the minimal possible number of iterations that produces reasonable results for photographic images with Gaussian noise for deblurring and denoising problems is $N = 30$ and $\mu = 0.8$.

IV. Experiments

Using an experimental approach, we have analyzed the effect of TGV applied to noisy images deblurred by BM3D algorithm.

A. Blur model

We have considered three types of blur corresponding to real out-of-focus blur in photographic images:

1. Gaussian blur

$$G_{\sigma}(x, y) = \frac{1}{2\pi\sigma^2} \exp\left(-\frac{x^2 + y^2}{2\sigma^2}\right)$$

2. Disk blur

$$D_r(x, y) = \begin{cases} 1, & x^2 + y^2 \le r^2, \\ 0, & \text{otherwise.} \end{cases}$$

3. Ring blur

$$R_r(x,y) = \begin{cases} 0.25, & x^2+y^2 \le 0.75r^2, \\ 1, & 0.75r^2 < x^2+y^2 \le r^2, \\ 0, & \text{otherwise.} \end{cases}$$

The examples of real out-of-focus blur are shown in Fig. 2. The kernels of modeled blur are shown in Fig. 3.

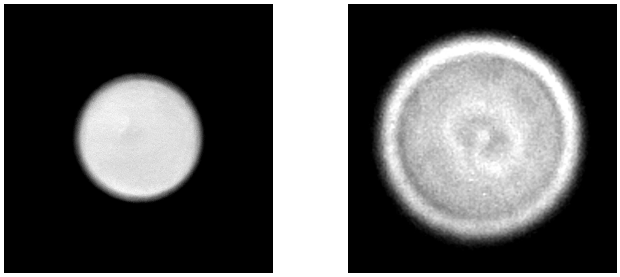

(a) Object is in front of the focal plane

(b) Object is behind the focal plane

Fig. 2. Examples of real out-of-focus blur kernels — images of small bright dot.

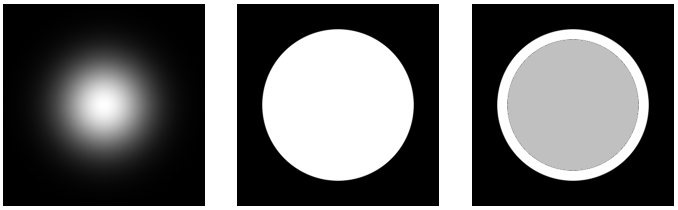

(a) Gaussian kernel (b) Disk kernel (c) Ring kernel

Fig. 3. Blur kernels used in the paper.

B. Scenario

Test images were generated using 24 natural images from TID2013 database [15]. Each reference image was convolved with Gaussian, disk and ring blur kernels with random blur parameter within $[1, 5]$ range. Gaussian white noise with random standard deviation in the range of $[0, 10]$ was added to each blurred image.

The images were deblurred and denoised by BM3D algorithm [8]. In practice, the blur kernel has to be estimated. We assume that the blur kernel type is known and its parameter allows up to 20% relative error.

Then we applied TGV algorithm with identity operator A in data fidelity term (2):

$$z_R = \arg\min_z \left(\|z-u\|_2^2 + \alpha_1 \|\nabla z\|_1 + \alpha_2 \|\nabla(\nabla z)\|_1 \right).$$

The regularization parameters α_1 and α_2 were chosen in order to maximize the SSIM value after denoising.

C. Results

The experiments have shown that application of GTV denoising after BM3D algorithm leads to image quality improvement. Strong TGV regularization tends to produce unnaturally looking image and fine detail loss while BM3D algorithm keeps some noise. A combined algorithm effectively suppress the noise without detail loss.

Some examples of the obtained results are shown in Fig. 4, Fig. 5 and Fig. 6.

(a) Reference image (b) Blurred and noisy image, PSNR = 22.58, SSIM = 0.5699

(c) TGV deblurring, PSNR = 26.77, SSIM = 0.8330 (d) BM3D deblurring, PSNR = 24.55, SSIM = 0.6944 (e) Proposed TGV after BM3D, PSNR = 27.21, SSIM = 0.8575

Fig. 4. Application of the proposed method to 'flower' image fragment with ring blur.

(a) Reference image (b) Blurred and noisy image, PSNR = 21.64, SSIM = 0.5428

(c) TGV deblurring, PSNR = 23.21, SSIM = 0.7572 (d) BM3D deblurring, PSNR = 23.29, SSIM = 0.7404 (e) Proposed TGV after BM3D, PSNR = 23.32, SSIM = 0.7612

Fig. 5. Application of the proposed method to 'lighthouse' image fragment with Gaussian blur.

V. Conclusion

In this paper a method based on Total Generalized Variation has been used to enhance the results of BM3D denoising and deblurring algorithm. The proposed combination gets the benefits of both TGV and BM3D algorithms by reducing the noise without loss of details. A computationally efficient

(a) Reference image

(b) Blurred and noisy image, PSNR = 22.66, SSIM = 0.5943

(c) TGV deblurring, PSNR = 25.85, SSIM = 0.8067

(d) BM3D deblurring, PSNR = 26.05, SSIM = 0.8020

(e) Proposed TGV after BM3D, PSNR = 26.11, SSIM = 0.8097

Fig. 6. Application of the proposed method to 'boat' image fragment with ring blur.

numerical algorithm for minimization of TGV regularization functional has been proposed.

Our implementation of TGV deblurring and denoising can be downloaded at http://imaging.cs.msu.ru/soft.

ACKNOWLEDGMENT

The work was supported by Russian Science Foundation Grant 17-11-01279.

REFERENCES

[1] L. I. Rudin, S. Osher, and E. Fatemi, "Nonlinear total variation based noise removal algorithms," *Physica D: nonlinear phenomena*, vol. 60, no. 1-4, pp. 259–268, 1992.

[2] T. Wang, Z. Qin, and M. Zhu, "An ELU network with total variation for image denoising," in *International Conference on Neural Information Processing*, 2017, pp. 227–237.

[3] M. V. Afonso and J. M. R. Sanches, "Blind inpainting using ℓ_0 and total variation regularization," *IEEE Transactions on Image Processing*, vol. 24, no. 7, pp. 2239–2253, 2015.

[4] J. Liu, T.-Z. Huang, I. W. Selesnick, X.-G. Lv, and P.-Y. Chen, "Image restoration using total variation with overlapping group sparsity," *Information Sciences*, vol. 295, pp. 232–246, 2015.

[5] K. Bredies, K. Kunisch, and T. Pock, "Total generalized variation," *SIAM Journal on Imaging Sciences*, vol. 3, no. 3, pp. 492–526, 2010.

[6] K. Bredies and T. Valkonen, "Inverse problems with second-order total generalized variation constraints," *Proceedings of SampTA*, vol. 201, 2011.

[7] V. Katkovnik, A. Foi, K. Egiazarian, and J. Astola, "From local kernel to nonlocal multiple-model image denoising," *International journal of computer vision*, vol. 86, no. 1, p. 1, 2010.

[8] A. Danielyan, V. Katkovnik, and K. Egiazarian, "BM3D frames and variational image deblurring," *IEEE Transactions on Image Processing*, vol. 21, no. 4, pp. 1715–1728, 2012.

[9] M. Matrecano, G. Poggi, and L. Verdoliva, "Improved BM3D for correlated noise removal." in *VISAPP (1)*, 2012, pp. 129–134.

[10] H. Yue, X. Sun, J. Yang, and F. Wu, "Image denoising by exploring external and internal correlations," *IEEE Transactions on Image Processing*, vol. 24, no. 6, pp. 1967–1982, 2015.

[11] F. Knoll, K. Bredies, T. Pock, and R. Stollberger, "Second order total generalized variation (TGV) for MRI," *Magnetic resonance in medicine*, vol. 65, no. 2, pp. 480–491, 2011.

[12] S. Farsiu, M. D. Robinson, M. Elad, and P. Milanfar, "Fast and robust multiframe super resolution," *IEEE Transactions on Image Processing*, vol. 13, no. 10, pp. 1327–1344, 2004.

[13] Y. Nesterov *et al.*, "Gradient methods for minimizing composite objective function," 2007.

[14] I. Sutskever, J. Martens, G. Dahl, and G. Hinton, "On the importance of initialization and momentum in deep learning," in *International conference on machine learning*, 2013, pp. 1139–1147.

[15] N. Ponomarenko, L. Jin, O. Ieremeiev, V. Lukin, K. Egiazarian, J. Astola, B. Vozel, K. Chehdi, M. Carli, F. Battisti, and C.-C. J. Kuo, "Image database TID2013: Peculiarities, results and perspectives," *Signal Processing: Image Communication*, vol. 30, pp. 57–77, 2015.